Available: https://doi.org/10.54117/jcddms.v4i1.58 *Research article*

Journal of Computational Drug Design and Molecular Simulations
J. Comput. Drug Des. Mol. Simul., 4(1): 91-103 (2026)
DOI: https://doi.org/10.54117/jcddms.v4i1.58

GC-MS Profiling and *In Silico* Evaluation of *Acalypha wilkesiana* Leaf Phytocompounds for Antimicrobial, Antioxidant, and Anti-Inflammatory Activity in Oral Health

Nwolisah, O. S.[1*], Okeugo, C. O.[2] and Enemor, V. H. A.[1]

[1]Department of Applied Biochemistry, Nnamdi Azikiwe University, P.M.B. 5025, Awka, Anambra State, Nigeria.
[2]Department of Biotechnology, Godfrey Okoye University, Enugu State, Nigeria.

*Corresponding author e-mail: ogenwolisah@gmail.com

Abstract

In many local communities, the leaves of *Acalypha wilkesiana* (Euphorbiaceae) are chewed to manage toothache and other dental inflammations. Despite this widespread ethnomedicinal practice, the phytochemical basis and molecular mechanisms underlying these oral health benefits remain poorly understood. This study aimed to identify the bioactive phytoconstituents in the ethanolic leaf extract of *A. wilkesiana* using gas chromatography-mass spectrometry (GC-MS) and to evaluate their antimicrobial, antioxidant, and anti-inflammatory potential through molecular docking, drug-likeness, and toxicity prediction. Ethanol extract of *A. wilkesiana* leaf was analyzed by GC-MS, and the identified compounds were subjected to molecular docking against four target proteins: *Streptococcus mutans* glucosyltransferase B (PDB: 8FJC), *Candida albicans* exo-1,3-beta-glucanase, human glutathione peroxidase, and cyclooxygenase-2. Drug-likeness was assessed using Lipinski and Veber rules, and toxicity was predicted using ProTox-II. Sixty two compounds were identified with squalene (21.13%), oleic acid (17.62%), and 13-octadecenal, (Z)- (16.63%) as the most abundant. Molecular docking revealed that Aspidospermidin-17-ol, 1-acetyl-19,21-epoxy-15,16-dimethoxy- exhibited the highest binding affinities against 8FJC (-7.8 kcal/mol), 2HE3 (-6.9 kcal/mol), and 3NTG (-7.6 kcal/mol), while cyclotetradecane, 1,7,11-trimethyl-4-(1-methylethyl)- showed the strongest binding to 4M81 (-9.6 kcal/mol). Drug-likeness analysis indicated that epinephrine, aspidospermidin-17-ol, 1-acetyl-19,21-epoxy-15,16-dimethoxy-, 7,9-di-tert-butyl-1-oxaspiro(4,5)deca-6,9-diene-2,8-dione, and dibutyl phthalate complied with Lipinski's rules. Toxicity prediction showed that most compounds fell within Classes IV–VI (low to non-toxic). No hepatotoxicity or mutagenicity was predicted for any phytocompound. The ethanolic leaf extract of *A. wilkesiana* contains a diverse array of bioactive compounds demonstrating promising activity against bacterial, antioxidant, and inflammatory proteins. These findings provide a scientific basis for the local practice of chewing *A. wilkesiana* leaves for dental relief and support further investigation of its lead compounds for phytodentistry applications.

Keywords: *Acalypha wilkesiana,* phytocompounds, gas chromatography-mass spectrometry, phytodentistry

Article History

Received: 25 Mar 2026
Accepted: 29 Apr 2026
Published: 10 May 2026

Scan QR code to view

How to cite this paper: Nwolisah, O. S., Okeugo, C. O., & Enemor, V. H. A. (2026). GC-MS Profiling and In Silico Evaluation of Acalypha wilkesiana Leaf Phytocompounds for Antimicrobial, Antioxidant, and Anti-Inflammatory Activity in Oral Health. *Journal of Computational Drug Design and Molecular Simulations*, *4*(1), 91–103. https://doi.org/10.54117/jcddms.v4i1.58

Introduction

Since ancient times, plant materials have been traditionally used in various forms, such as chewing sticks, latex or exudates, tooth powders, or mouth rinses, to maintain oral hygiene, prevent dental diseases, and promote overall dental health (Isola, 2020). Medicinal plants have been shown to possess a broad and specific spectrum of biological activities, including antimicrobial, antioxidant, anti-inflammatory, antifungal, antiviral, and analgesic effects relevant to oral health (Isola, 2020; Milutinovici *et al.*, 2021). The recent emergence of phytodentistry, an alternative therapeutic approach that harnesses the medicinal properties of plants and herbs to manage a variety of oral conditions, offers a potentially safe and cost-effective alternative to synthetic drugs (Moghadam *et al.*, 2020). One such plant with ethnomedicinal relevance to oral health is *Acalypha wilkesiana* (Euphorbiaceae). This tropical shrub is commonly used in traditional medicine to manage various inflammatory and infectious conditions, with local practices reporting its use for treating toothache and dental inflammations. Dental caries, primarily associated with oral microbial pathogens are caused by microbial infections (Kouidhi *et al.*, 2010). Among the key bacterial pathogens, *Streptococcus mutans* plays a central role

by initiating biofilm formation on tooth surfaces through glucan synthesis mediated by the enzyme glucosyltransferase (GtfB) (Bowen and Koo, 2011).

Previous studies have reported the presence of essential vitamins such as C and E in the leaves of *A. wilkesiana* (Nwolisah *et al.*, 2024). These micronutrients are particularly relevant to oral health, as Vitamin C is critical for collagen synthesis in the gums and periodontal ligament and has been strongly associated with a reduced risk of periodontal disease (Ustianowski *et al.*, 2023; Mi *et al.* 2024), while Vitamin E exerts anti-inflammatory effects through the inhibition of COX-2 and has shown benefits in managing periodontal parameters (Mi *et al.* 2024). These nutritional findings, coupled with the plant's ethnomedicinal uses, suggest that *A. wilkesiana* may harbor a broader range of bioactive compounds with therapeutic potential for oral health. However, the biological basis for these dental-related applications has not been fully elucidated.

Therefore, the present study aimed to identify the phytochemical constituents of the ethanolic leaf extract using GC-MS and evaluate their potential as antimicrobial, antioxidant, and anti-inflammatory agents through molecular docking. The findings will help validate the ethnomedicinal use of *A. wilkesiana* in oral care and identify potential lead compounds for the development of phytodentistry-based therapeutics.

Materials and Method

Chemicals and Reagents

All reagents and chemicals used were of standard analytical grade, and were products of British Drug House (BDH), England; May and Baker, England; Sigma Aldrich, USA.

Collection and Preparation of Plant Materials

Fresh *Acalypha wilkesiana* leaves were collected from a garden in Agbor quarters, Alor, in Idemili South Local Government Area, Anambra State. The plant sample was deposited, identified and authenticated (with voucher number: NAUH-241[a]) by the Curator of the herbarium, of the Department of Botany, Faculty of Biosciences, Nnamdi Azikiwe University Awka. The freshly collected leaves were thoroughly washed in running tap water and rinsed in distilled water, shade-dried at room temperature (25˚C) for 10 days. The leaves were ground to powder and preserved in an air tight bottle.

Extraction of Phytochemicals

One gram (1 g) of the leaf sample was weighed and transferred into a test tube and 25 ml of ethanol was added. The test tube was heated on a hot plate at 60°C for 90 minutes. After the reaction time, the reaction product contained in the test tube was transferred to a separatory funnel. The tube was washed with 20 ml of ethanol, 10 ml of cold water, 10 ml of hot water and 3 ml of hexane, which were all transferred to the funnel. These extracts were combined and washed three times with 10 ml of an aqueous 10 % v/v ethanol solution. The solution was dried with anhydrous sodium sulfate, and the solvent was removed by evaporation. The sample was solubilized in 1000 µl of pyridine of which 200 µl was transferred to a vial for analysis.

Gas Chromatography-Mass Spectrometry (GC-MS) Analysis

The analysis of the phytochemicals was performed on a BUCK M910 gas chromatograph equipped with HP-5MS column (30 m in length × 250 µm in diameter × 0.25 µm in film thickness). Spectrometric detection by GC–MS involved an electron ionization system which utilized high energy electrons (70 eV). Pure helium gas (99.995 %) was used as the carrier gas with flow rate of 1 mL/min. The initial temperature was set at 50 °C, with a heating rate of 3 °C/min, and a holding time of about 10 minutes. Finally, the temperature was increased to 300 °C at 10 °C/min. One microliter (1 µl) of the prepared 1% of the extract diluted with acetonitrile was injected in a splitless mode. The relative amounts of the chemical compounds in each extracts were expressed as percentages based on the peak areas in the chromatogram. Bioactive compounds extracted from the ethanol extract were identified based on GC retention time on an HP-5MS column and by matching spectra with computer software data for standards (Replib and Mainlab data of GC–MS systems). The peaks correspond to bioactive compounds identified by correlating their peak retention time, peak area (%), and mass spectral fragmentation patterns with known compounds in the National Institute of Standards and Technology (NIST) library.

Molecular Docking

Ligand preparation

All the structural data of the phytochemicals were downloaded from PubChem. Structure files were converted to protein data bank format using Open Babel.

Protein target preparation

The x-ray crystal structure data of the catalytic domain of *Streptococcus mutans* Glucose transferase B (GtfB) (PDB ID: 8FJC), E292s glycosynthase variant of exo-1,3-beta-glucanase from *Candida albicans* (PDB ID: 4M81), the selenocysteine to cysteine mutant of human glutathionine peroxidase 2 (GPX2) (PDB ID: 2HE3), and crystal structure of COX-2 with selective compound 23d-(R) (PDB ID: 3NTG) were downloaded from the Research Collaboratory for Structural Bioinformatics (RCSB) database (http:// www.rcsb.org/pdb). Target selection was based on documented roles in oral microbial pathogenicity and periodontal inflammatory pathways. All the target proteins and ligands were docked using PyRx. The best binding conformation of phytocompounds against target proteins was determined to be the one with the lowest total binding energy. Furthermore, the detailed 2D and 3D detailed interactions between the best phytocompound identifed and its binding sites on the target proteins were visualized in Biovia Discovery Studio.

Absorption Distribution Metabolism and Excretion (ADME) Screening and Drug- Likeness Prediction

The *in silico* ADME screening and drug-likeness evaluation were performed using SwissADME (http://swissadme.ch). The lead compounds were subjected to this part of the screening process. Simple physicochemical properties, including molecular weight (MW), atom counts, and polar surface area (PSA) were computed. Drug-likeness candidature was implemented by Lipinski (2001), and Veber (2002) rules of 5 (RO5) screening.

Toxicity Prediction

The toxicological properties of the bioactive compounds of *A. wilkesiana* leaf were predicted using ProTox-II webserver (http://tox.charite.de/protox_II/) for *in-silico* toxicity prediction.

Results

GC-MS Phytochemical Analysis of Acalypha wilkesiana Leaf Sample

The analysis identified 62 compounds in the ethanol leaf extract of *A. wilkesiana* (Table 1). The GC-MS chromatogram of the ethanol leaf extract of *Acalypha wilkesiana* displayed a total of 62 peaks (Fig. 1).

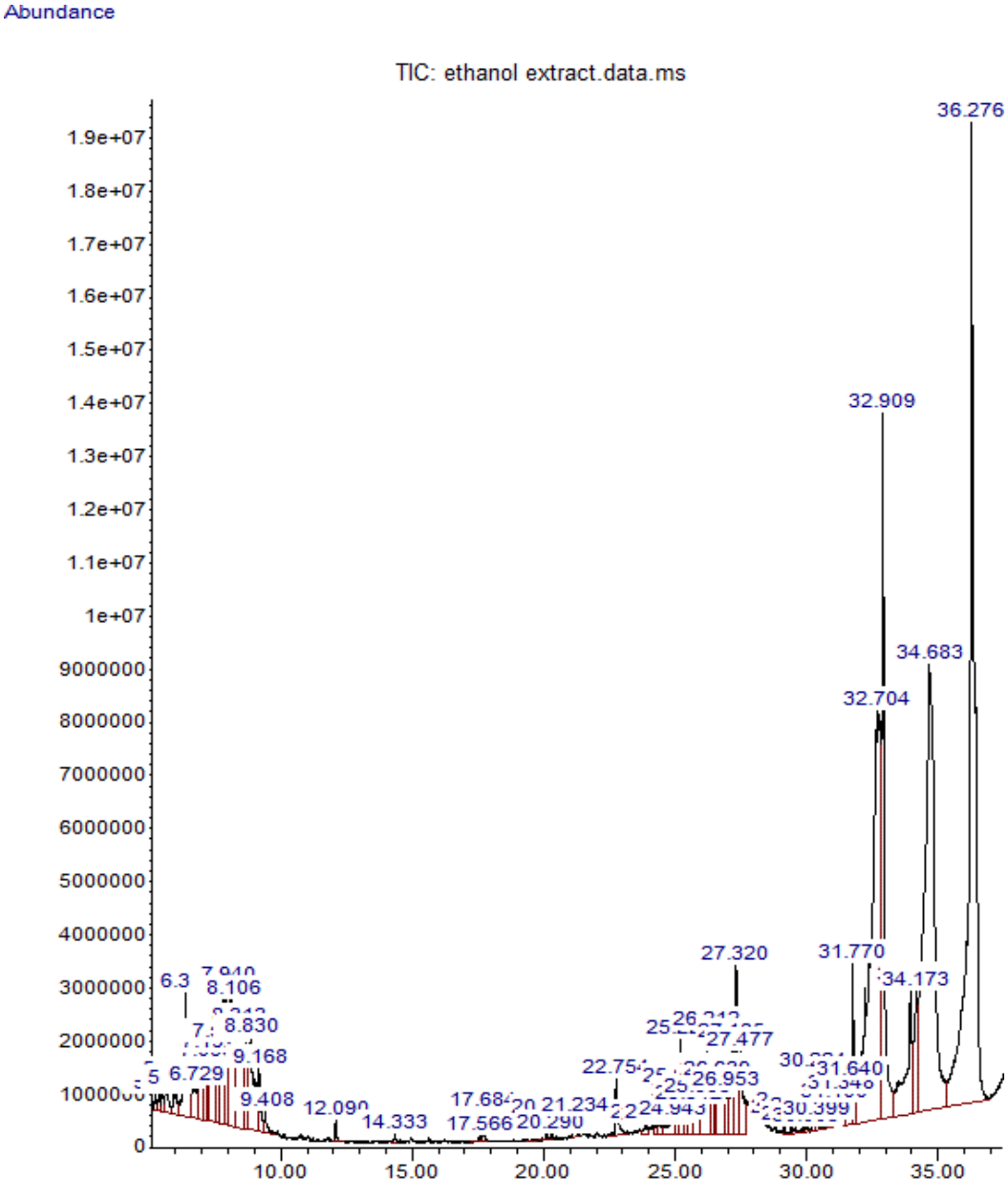

Figure 1: Chromatogram of phytoconstituents detected in the ethanol leaf extract of *A. wilkesiana*

Table 1: Compounds identified from the ethanolic extract of *Acalypha wilkesiana* by GC-MS analysis.

S/N	Compound	Molecular formula	Class of compound	Retention time (min)	Area (%)
1	4-Heptafluorobutyryloxyhexadecane	$C_{20}H_{33}F_7O_2$	Fluorinated ester	5.214	0.09
2	3-Tetradecene, (E)-	$C_{14}H_{28}$	Alkene	5.367	0.13
3	Benzene, 1-ethyl-3-methyl-	C_9H_{12}	Aromatic hydrocarbon	5.479	0.23
4	Benzene, 1,2,3-trimethyl-	C_9H_{12}	Aromatic hydrocarbon	5.686	0.36
5	Cycloheptane, methyl-	C_8H_{16}	Cycloalkane	5.930	0.39
6	Decane	$C_{10}H_{22}$	Alkane	6.367	1.44
7	5-Eicosene, (E)-	$C_{20}H_{40}$	Alkene	6.729	0.56
8	E-15-Heptadecenal	$C_{17}H_{32}O$	Aldehyde (unsaturated)	6.967	0.67
9	Dichloroacetic acid, 2-pentadecylester	$C_{17}H_{30}C_{l2}O_2$	Halogenated ester	7.093	0.63
10	4-Propylcyclohexanone	$C_9H_{16}O$	Ketone	7.192	0.49
11	1-Fluorononane	$C_9H_{19}F$	Haloalkane	7.409	1.57
12	Cyanoacetic acid, tetradecyl ester	$C_{17}H_{31}NO_2$	Nitrile ester	7.583	0.78
13	Naphthalene, decahydro-, trans-	$C_{10}H_{18}$	Bicyclic hydrocarbon	7.815	2.05
14	Decane, 1-fluoro-	$C_{10}H_{21}F$	Haloalkane	7.940	1.12
15	2-Trifluoroacetoxytridecane	$C_{15}H_{27}F_3O_2$	Fluorinated ester	8.106	2.30
16	Oxalic acid, allyl undecyl ester	$C_{16}H_{28}O_4$	Di-ester	8.313	2.14
17	1-Nonadecene	$C_{19}H_{38}$	Alkene	8.672	1.01
18	Pentadec-7-ene, 7-bromomethyl-	$C_{16}H_{31}Br$	Brominated alkene	8.830	2.08
19	Undecane	$C_{11}H_{24}$	Alkane	9.168	0.57
20	Naphthalene, decahydro-2-methyl-	$C_{11}H_{20}$	Bicyclic hydrocarbon	9.408	0.22
21	Dodecane	$C_{12}H_{26}$	Alkane	12.090	0.13
22	Heptadecane, 8-methyl-	$C_{18}H_{38}$	Branched alkane	14.333	0.04
23	7-Tetradecene, (E)-	$C_{14}H_{28}$	Alkene	17.566	0.04
24	Tetradecane	$C_{14}H_{30}$	Alkane	17.684	0.20
25	Heptadecane	$C_{17}H_{36}$	Alkane	20.101	0.10
26	Hentriacontane	$C_{31}H_{64}$	Long-chain alkane	20.290	0.05
27	Eicosane, 1-iodo-	$C_{20}H_{41}I$	Haloalkane	21.234	0.22
28	Hexadecane	$C_{16}H_{34}$	Alkane	22.754	0.59
29	Epinephrine	$C_9H_{13}NO_3$	Catecholamine	23.877	0.13
30	Tetrapentacontane, 1,54-dibromo-	$C_{54}H_{108}Br_2$	Dihaloalkane	24.243	0.08
31	Hexadecane, 1-(ethenyloxy)-	$C_{18}H_{36}O$	Ether	24.400	0.15
32	7-Methyl-Z-tetradecen-1-ol acetate	$C_{17}H_{32}O_2$	Ester (acetate)	24.943	0.38
33	Dodecane, 2-methyl-	$C_{13}H_{28}$	Branched alkane	25.095	0.40
34	Heptadecane	$C_{17}H_{36}$	Alkane	25.222	0.81
35	Oxalic acid, 3,5-difluorophenyl tetradecyl ester	$C_{22}H_{32}F_2O_4$	Aromatic ester	25.427	0.26
36	Aspidospermidin-17-ol, 1-acetyl-19,21-epoxy-15,16-dimethoxy-	$C_{24}H_{30}N_2O_6$	Indole alkaloid	25.542	0.41
37	Oleic Acid	$C_{18}H_{34}O_2$	Fatty acid (monounsaturated)	25.895	0.71
38	Eicosane	$C_{20}H_{42}$	Alkane	26.212	1.71
39	Octadecane	$C_{18}H_{38}$	Alkane	26.411	0.49
40	1-Octadecanesulphonyl chloride	$C_{18}H_{37}ClO_2S$	Sulfonyl chloride	26.497	0.47
41	2-Methylhexacosane	$C_{27}H_{56}$	Branched alkane	26.639	1.30
42	Heptadecane, 3-methyl-	$C_{18}H_{38}$	Branched alkane	26.953	0.43
43	5-Eicosene, (E)-	$C_{20}H_{40}$	Alkene	27.185	1.05
44	Octadecane	$C_{18}H_{38}$	Alkane	27.320	1.36
45	5-Octadecene, (E)-	$C_{18}H_{36}$	Alkene	27.477	1.16
46	Nonadecane	$C_{19}H_{40}$	Alkane	29.151	0.07
47	Eicosane	$C_{20}H_{42}$	Alkane	29.391	0.09
48	7,9-Di-tert-butyl-1- oxaspiro(4,5)deca-6,9-diene-2,8-dione	$C_{17}H_{24}O_3$	Phenolic antioxidant derivative	29.574	0.07
49	Nonane, 5-butyl-	$C_{13}H_{28}$	Branched alkane	29.887	0.08
50	Dibutyl phthalate	$C_{16}H_{22}O_4$	Phthalate ester	30.003	0.05
51	1-Octadecene	$C_{18}H_{36}$	Alkene	30.224	0.33
52	E-15-Heptadecenal	$C_{17}H_{32}O$	Aldehyde	30.399	0.06
53	Heptadecane, 2-methyl-	$C_{18}H_{38}$	Branched alkane	31.100	0.37
54	Octadecane, 3-methyl-	$C_{19}H_{40}$	Branched alkane	31.348	0.33
55	Cyclotetradecane, 1,7,11- trimethyl-4-(1-methylethyl)-	$C_{20}H_{40}$	Cycloalkane	31.640	0.59
56	1-Docosene	$C_{22}H_{44}$	Alkene	31.770	0.87
57	13-Octadecenal, (Z)-	$C_{18}H_{34}O$	Aldehyde	32.704	16.63
58	Carbonic acid, but-2-yn-1-yl eicosyl ester	$C_{25}H_{46}O_3$	Carbonate ester	32.909	5.98
59	Bis(tridecyl) phthalate	$C_{34}H_{58}O_4$	Phthalate ester	33.949	2.95
60	1-Hexacosene	$C_{26}H_{52}$	Alkene	34.173	1.35
61	9-Octadecenoic acid (Z)-	$C_{18}H_{34}O_2$	Fatty acid (monounsaturated)	34.683	17.62
62	Squalene	$C_{30}H_{50}$	Triterpene (isoprenoid)	36.276	21.13

Molecular Docking

The molecular docking results, presented as minimum binding energy values (kcal/mol), are shown in Table 2. The phytocompounds exhibited varying binding affinities across the four target proteins. Against the bacterial protein (8FJC), binding energies ranged from -3.9 to -7.8 kcal/mol, while scores against the fungal protein (4M8I) ranged from -3.2 to -9.6 kcal/mol. For the antioxidant protein (2HE3), binding energies ranged from -3.1 to -6.9 kcal/mol, and against the pro-inflammatory protein (3NTG), scores ranged from -3.2 to -7.6 kcal/mol.

The five compounds with the highest binding affinities were selected for each target protein. Against the bacterial protein (8FJC), the top-ranking compound was Aspidospermidin-17-ol, 1-acetyl-19,21-epoxy-15,16-dimethoxy- with a binding energy of -7.8 kcal/mol, followed by 7,9-Di-tert-butyl-1-oxaspiro(4,5)deca-6,9-diene-2,8-dione, Cyclotetradecane, 1,7,11-trimethyl-4-(1-methylethyl)-, Squalene, and 4-Heptafluorobutyryloxyhexadecane. For the fungal protein (4M8I), Cyclotetradecane, 1,7,11-trimethyl-4-(1-methylethyl)- exhibited the highest binding affinity at -9.6 kcal/mol, followed by Aspidospermidin-17-ol, 1-acetyl-19,21-epoxy-15,16-dimethoxy-, 7,9-Di-tert-butyl-1-oxaspiro(4,5)deca-6,9-diene-2,8-dione, Squalene, and 4-Heptafluorobutyryloxyhexadecane.

Against the antioxidant protein (2HE3), Aspidospermidin-17-ol, 1-acetyl-19,21-epoxy-15,16-dimethoxy- again showed the highest binding energy at -6.9 kcal/mol, followed by Oxalic acid, 3,5-difluorophenyl tetradecyl ester, 7,9-Di-tert-butyl-1-oxaspiro(4,5)deca-6,9-diene-2,8-dione, Cyclotetradecane, 1,7,11-trimethyl-4-(1-methylethyl)-, and Epinephrine. For the pro-inflammatory protein (3NTG), Aspidospermidin-17-ol, 1-acetyl-19,21-epoxy-15,16-dimethoxy- recorded the highest binding affinity at -7.6 kcal/mol, followed by Squalene, Naphthalene, decahydro-2-methyl-, Heptadecane, 3-methyl-, and Bis(tridecyl) phthalate (Figs. 2-5).

Table 2: Binding energy values (ΔG- Kcal/mol) of the phytocompounds of *A. wilkesiana* leaf, compared with the standard drugs.

Compounds	8FJC (Kcal/mol)	4M81 (Kcal/mol)	2HE3 (Kcal/mol)	3NTG (Kcal/mol)
4-Heptafluorobutyryloxyhexadecane	-6.5	-7.8	-5.0	-6.4
3-Tetradecene, (E)-	-4.4	-6.3	-3.9	-5.7
Benzene, 1-ethyl-3-methyl-	-5.4	-6.4	-4.6	-5.9
Benzene, 1,2,3-trimethyl-	-5.6	-5.9	-4.6	-6.0
Cycloheptane, methyl-	-4.3	-5.6	-4.7	-5.9
Decane	-4.6	-5.3	-3.7	-5.3
5-Eicosene, (E)-	-5.2	-6.4	-3.9	-4.6
E-15-Heptadecenal	-5.2	-6.5	-4.4	-5.2
Dichloroacetic acid, 2-pentadecyl ester	-4.4	-6.7	-4.0	-5.9
4-Propylcyclohexanone	-4.9	-6.0	-4.6	-6.3
1-Fluorononane	-4.2	-5.2	-3.7	-4.8
Cyanoacetic acid, tetradecyl ester	-5.3	-6.1	-4.8	-5.5
Naphthalene, decahydro-, trans-	-6.0	-6.6	-4.9	-6.8
Decane, 1-fluoro-	-4.1	-5.2	-3.7	-5.4
2-Trifluoroacetoxytridecane	-5.6	-7.1	-4.9	-5.9
Oxalic acid, allyl undecyl ester	-4.8	-6.4	-4.9	-6.1
1-Nonadecene	-4.5	-6.7	-5.0	-4.3
Pentadec-7-ene, 7-bromomethyl-	-4.9	-6.8	-4.6	-5.1
Undecane	-4.6	-5.6	-3.8	-5.3
Naphthalene, decahydro-2-methyl-	-6.2	-7.1	-5.0	-7.0
Dodecane	-4.8	-5.8	-3.9	-5.6
Heptadecane, 8-methyl-	-5.2	-6.9	-4.6	-4.8
7-Tetradecene, (E)-	-5.2	-6.2	-3.6	-5.6
Tetradecane	-4.9	-6.0	-4.2	-5.4
Heptadecane	-4.9	-6.3	-4.6	-5.1
Hentriacontane	-5.2	-6.7	-4.4	-4.3
Eicosane, 1-iodo-	-3.9	-6.4	-4.7	-5.9
Hexadecane	-5.0	-6.1	-4.2	-5.4
Epinephrine	-6.2	-6.4	-5.2	-6.4
Tetrapentacontane, 1,54-dibromo-	-4.5	-3.2	-4.6	-3.2
Hexadecane, 1-(ethenyloxy)-	-5.4	-6.1	-3.8	-5.0
7-Methyl-Z-tetradecen-1-ol acetate	-5.5	-6.9	-5.0	-5.5
Dodecane, 2-methyl-	-4.8	-6.1	-3.9	-5.8
Oxalic acid, 3,5-difluorophenyl tetradecyl ester	-6.4	-7.7	-5.6	-6.5
Aspidospermidin-17-ol, 1-acetyl-19,21-epoxy-15,16-dimethoxy-	-7.8	-8.8	-6.9	-7.8

Oleic Acid	-5.5	-6.9	-5.1	-5.7
Eicosane	-4.8	-6.4	-4.2	-5.6
Octadecane	-5.0	-6.1	-4.5	-4.0
1-Octadecanesulphonyl chloride	-5.3	-5.7	-3.6	-4.3
2-Methylhexacosane	-5.3	-3.2	-4.4	-6.4
Heptadecane, 3-methyl-	-4.9	-6.5	-4.7	-6.9
5-Octadecene, (E)-	-4.2	-6.8	-4.5	-4.8
Nonadecane	-4.9	-6.4	-4.3	-3.8
7,9-Di-tert-butyl-1-oxaspiro(4,5)deca-6,9-diene-2,8-dione	-7.1	-8.7	-5.6	-6.4
Nonane, 5-butyl-	-5.0	-5.8	-3.8	-5.6
Dibutyl phthalate	-5.8	-7.5	-4.9	-6.4
1-Octadecene	-3.9	-6.5	-4.4	-4.2
Heptadecane, 2-methyl-	-5.8	-6.5	-4.6	-6.3
Octadecane, 3-methyl-	-4.9	-6.6	-4.7	-5.6
Cyclotetradecane, 1,7,11-trimethyl-4-(1-methylethyl)-	-6.9	-9.6	-5.6	-6.6
1-Docosene	-5.2	-3.6	-4.0	-3.8
13-Octadecenal, (Z)-	-5.1	-6.4	-4.9	-5.3
Carbonic acid, but-2-yn-1-yl eicosyl ester	-5.7	-4.5	-3.5	-4.0
Bis(tridecyl) phthalate	-6.4	-7.2	-5.0	-6.9
1-Hexacosene	-4.9	-6.6	-3.1	-4.3
9-Octadecenoic acid (Z)-	-5.8	-7.0	-4.8	-4.0
Squalene	-6.5	-8.6	-5.0	-7.4
Gentamicin (Control)	-7.4	-	-	-
Fluconazole (Control)	-	-8.1	-	-
Butylhydroxyanisole (Control)	-	-	-5.0	-
Celecoxib (Control)	-	-	-	-7.7

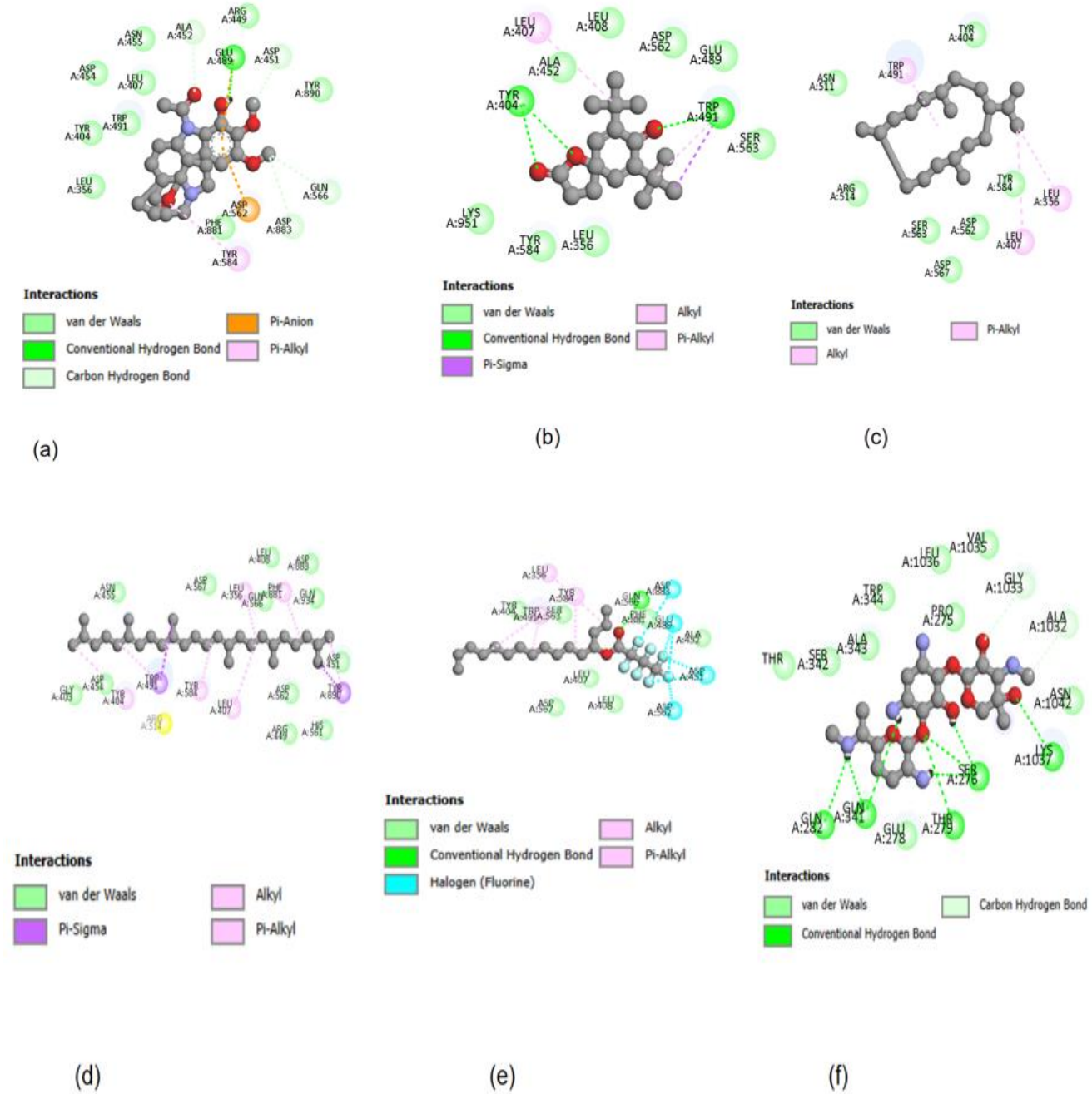

Figure 2: 2D representations of the best docking scores between x-ray crystal structure data of the catalytic domain of *Streptococcus mutans* GtfB (PDB ID: 8FJC) and (a) Aspidospermidin-17-ol, 1-acetyl- 19, 21-epoxy-15,16-dimethoxy-: conventional hydrogen bond (GLU-489), carbon hydrogen bond (ASP-562, GLN-566, ASP-451, ALA-452), π-alkyl bond (TYR-584), pi-anion bond (ASP-562); (b) 7,9-Di-tert-butyl-1- oxaspiro (4,5) deca-6,9-diene-2,8-dione: conventional hydrogen bond (TYR-404, TRP-491), and alkyl and π-alkyl bond (LEU-407); (c) Cyclotetradecane, 1,7,11-trimethyl-4-(1-methylethyl)-: akyl and π-alkyl bond (LEU-407, LEU-356, TRP-491); (d) Squalene: alkyl and π-alkyl bond (TYR-404, LEU-407, TRP-491, LEU-356, PHE-881), and π-sigma bond (TYR-890, TRP-491); (e) 4-Heptafluorobutyryloxyhexadecane: conventional hydrogen bond (GLN-566), halogen bond (ASP-562, ASP-451, ASP-883, GLU-489), alkyl and π-alkyl bond (LEU-366, TYR-584, TRP-491); (f) Gentamicin (control): conventional hydrogen bond (ASN-1042, LYS-1O37, SER-276, THR-279, GLN-341, GLN-282).

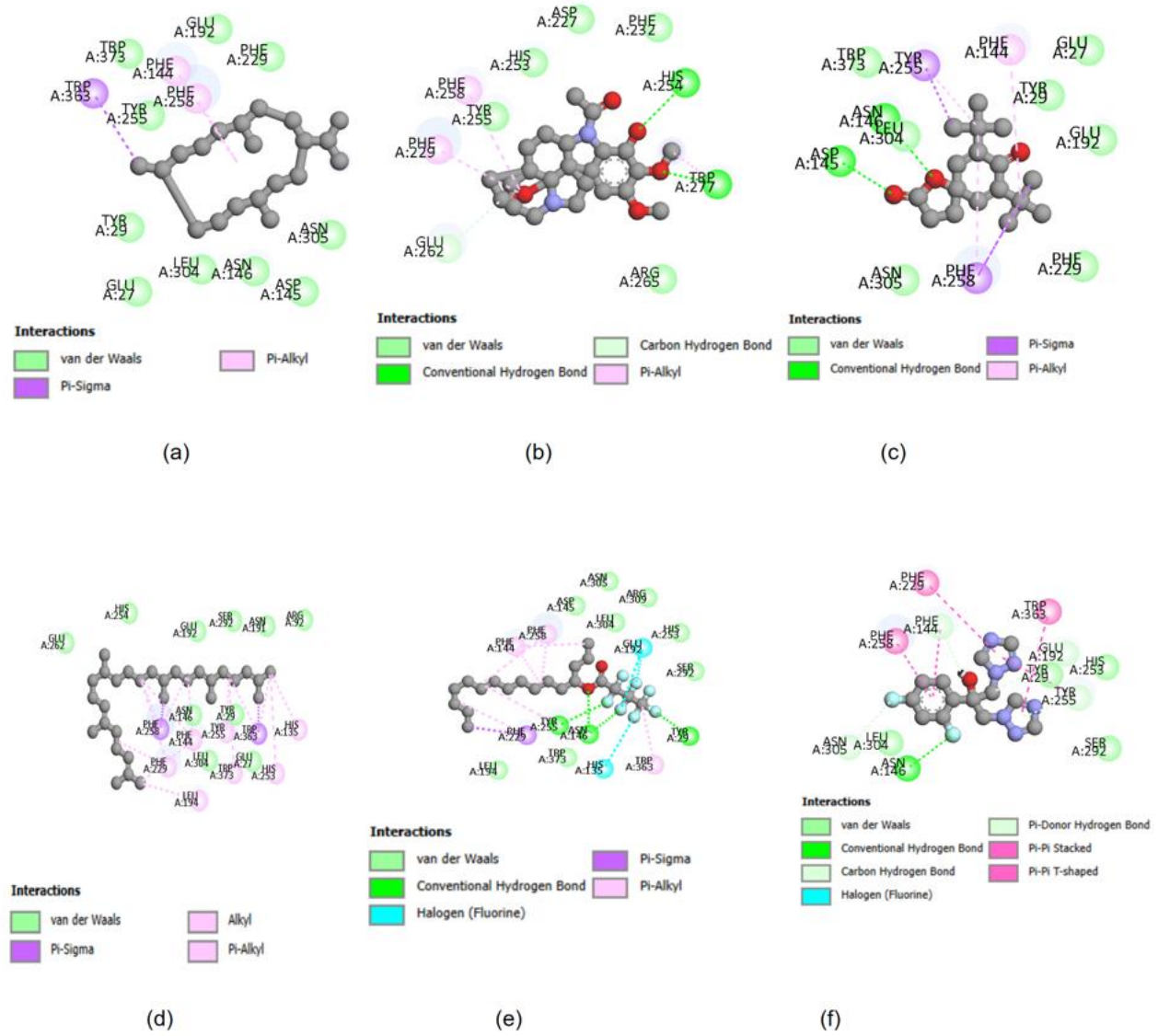

Figure 3: 2D representations of the best docking scores between E292s glycosynthase variant of exo-1,3-beta-glucanase from *Candida albicans* (PDB ID: 4M81) and (a) Cyclotetradecane, 1,7,11-trimethyl-4-(1-methylethyl)-: π-alkyl bond (PHE- 144, PHE-258), and π-sigma bond (TRP-363); (b) Aspidospermidin-17-ol, 1-acetyl- 19, 21-epoxy-15,16-dimethoxy-: conventional hydrogen bond (HIS-254, TRP-277), and π-alkyl bond (PHE-258, PHE-229); (c) 7,9-Di-tert-butyl-1- oxaspiro (4,5) deca-6,9-diene-2,8-dione: conventional hydrogen bond (ASN-146, ASP-145), π-alkyl bond (PHE-144, PHE -258, TYR-255), π-sigma bond (PHE-258, TYR-255); (d) Squalene: alkyl and π-alkyl bond (HIS-135, HIS-233, TRP-373, TYR-255, PHE-144, LEU-194, PHE-229), and π-sigma bond (TRP-363, PHE-258); (e) 4-Heptafluorobutyryloxyhexadecane: conventional hydrogen bond (TYR-255, ASN-146, TYR-29), halogen bond (GLU-192, HIS-135), π-alkyl bond (PHE-144, PHE-258, TYR-255, TRP-363), π-sigma bond (PHE-229); (f) fluconazole (control): conventional hydrogen bond (ASN -146), carbon hydrogen bond and pi-donor hydrogen bond (ASN-305, PHE-144, TYR-255), π-π stacked and π-π T-shaped bond (PHE-229, TRP-363, PHE-258, PHE -144).

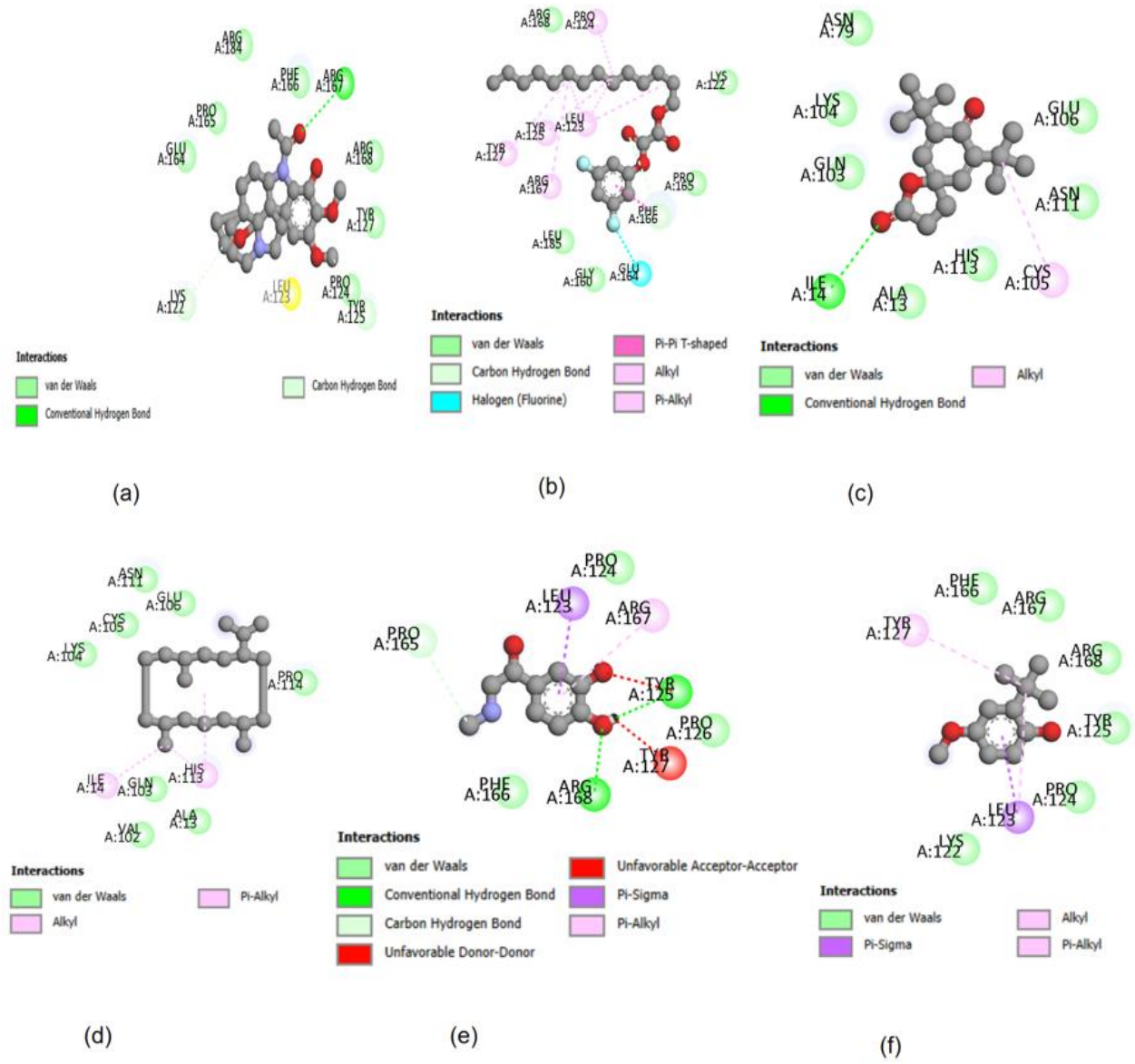

Figure 4: 2D representations of the best docking scores between the selenocysteine to cysteine mutant of human glutathionine peroxidase 2 (GPX2) (PDB ID: 2HE3) and (a) Aspidospermidin-17-ol, 1-acetyl- 19, 21-epoxy-15,16-dimethoxy-: conventional hydrogen bond (ARG-167), van der Waals (PRO-124), and carbon hydrogen bond (LYS-122); (b) Oxalic acid, 3,5-difluorophenyl tetradecyl ester: carbon hydrogen bond (PHE-166), halogen bond (GLU-164), alkyl and π-alkyl bond (PRO-124, LEU-123, TYR-125, TYR-127, ARG-167) π-π T-shaped bond (PHE-166); (c) 7,9-Di-tert-butyl-1- oxaspiro (4,5) deca-6,9-diene-2,8-dione: carbon hydrogen bond (ILE-14), alkyl bond (CYS-105); (d) Cyclotetradecane, 1,7,11-trimethyl-4-(1-methylethyl)-: alkyl and π-alkyl bond (HIS-113, ILE-14); (e) epinephrine: conventional hydrogen bond (TYR-125, ARG-168), π-sigma bond (LEU-123), π-alkyl bond (ARG-167), and unfavorable donor-donor and unfavorable acceptor-acceptor (TYR-125, TYR-127); (f) Butylhydroxyanisole (control): π-sigma bond (LEU-123), alkyl and π-alkyl bond (TYR-127)

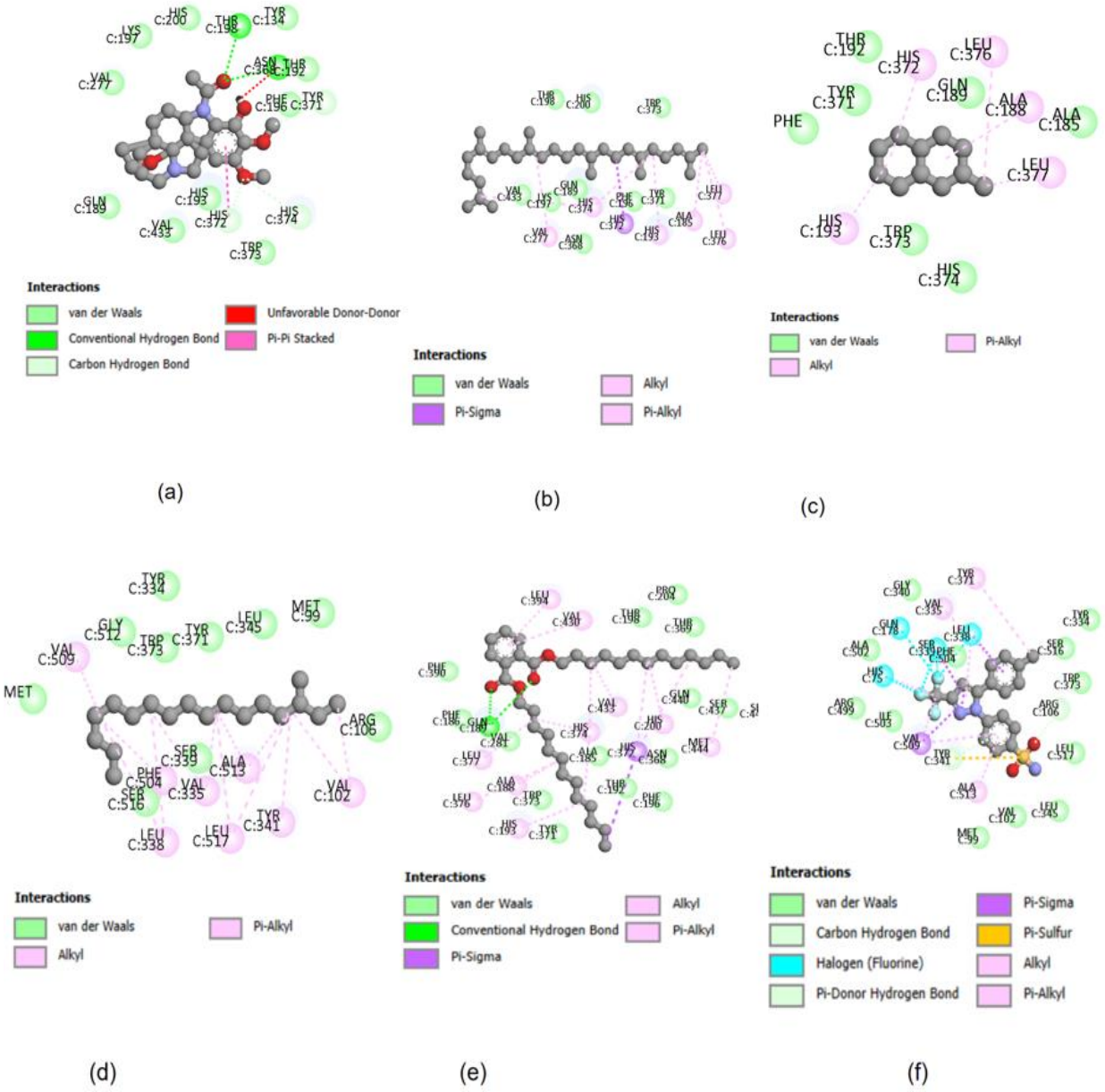

Figure 5: 2D representations of the best docking scores between crystal structure of COX-2 with selective compound 23d-(R) (PDB ID: 3NTG) and (a) Aspidospermidin-17-ol, 1-acetyl- 19, 21-epoxy-15,16-dimethoxy-: conventional hydrogen bond (ASN-368, THR-198), π-π stacked bond (HIS-372), carbon hydrogen bond (HIS-372, HIS-374), and unfavorable donor-donor (ASN-368); (b) Squalene: alkyl and π-alkyl bond (LEU-377, LEU-376, ALA-185, HIS-193, HIS-374, VAL-277), π-sigma bond (HIS-372); (c) Naphthalene, decahydro-2- methyl-: alkyl and π-alkyl bond (LEU-377, LEU-376, ALA-188, HIS-193, HIS-372); (d) Heptadecane, 3-methyl-: alkyl and π-alkyl bond (VAL-102, TYR-341, ALA-513, LEU-517, PHE 504, LEU-338, VAL-509); (e) Bis(tridecyl) phthalate: conventional hydrogen bond (GLN-189), π-sigma bond (HIS 372), alkyl and π-alkyl bond (LEU-394, VAL-430, MET-444, HIS-200, VAL-433, HIS-374, ALA-188, HIS-193, ALA-188, LEU-376, HIS-374); (f) Celecoxib (control): carbon hydrogen and pi-donor hydrogen bond (TYR-341), π-sigma bond (VAL-509, SER-339, LEU-338), halogen (LEU-338, GLN-178, HIS-75, SER-339), π-alkyl and alkyl bond (TYR-371, VAL-335, ALA-513, LEU-338, VAL-509).

ADME Evaluation

The compounds with the best binding affinities were selected for further ADME evaluation. Table 3 shows the physicochemical characteristics of the isolated compounds from *A. wilkesiana* leaf. The phytocompounds were assessed for drug-likeness properties and adherence to Lipinski's rule of five (RO5) and Veber rule.The molecular weights of the lead compounds ranged from 138.25 to 530.82 g/mol. The number of hydrogen bond acceptors and hydrogen bond donors for the compounds ranged from 0 to 9, and 0 to 4, respectively. The computed consensus lipophilicity values (LogPo/w) for the compounds ranged from 0.10 to 9.90. Epinephrine, aspidospermidin-17-ol,1-acetyl-19,21- epoxy-15,16-dimethoxy, 7,9-di-tert-butyl-1-oxaspiro(4,5)deca-6,9-diene-2,8-dione, and dibutyl phthalate adhered to all five rules of Lipinski without any violations. However, the other compounds violated at least one of the drug-likeness filters. The number of rotatable bonds varied from 0 to 28.

Table 3: Physicochemical properties associated with good oral bioavailability for the isolated compounds from *A. wilkesiana* leaf.

		Lipinski rules				Veber rules	
Compounds	M. W (g/mol) <500	HBA <10	HBD <5	Log*P* ≤5	Lipinski's Violation ≤1	nRB ≤10	TPSA ≤140Å²
4-Heptafluorobutyryloxyhexadecane	438.46	9	0	8.10	1	18	26.30
Naphthalene, decahydro-, trans-	138.25	0	0	3.64	1	0	0.00
Naphthalene, decahydro-2-methyl-	152.28	0	0	3.84	1	0	0.00
Epinephrine	183.20	4	4	0.10	0	3	72.72
Oxalic acid, 3,5-difluorophenyl tetradecyl Ester	398.48	6	0	6.70	1	17	52.60
7-Methyl-Z-tetradecen-1-ol acetate	268.43	2	0	5.09	1	13	26.30
Aspidospermidin-17-ol, 1-acetyl-19,21-epoxy-15,16-dimethoxy-	414.49	6	1	2.37	0	3	71.47
Oleic Acid	282.46	2	1	5.71	1	15	37.30
7,9-Di-tert-butyl-1-oxaspiro(4,5)deca-6,9-diene-2,8-dione	276.32	3	0	3.40	0	2	43.37
Dibutyl phthalate	278.34	4	0	3.69	0	10	52.60
Cyclotetradecane,1,7,11 trimethyl-4-(1-methylethyl)-	280.53	0	0	6.83	1	1	0.00
Bis(tridecyl) phthalate	530.82	4	0	9.90	2	28	52.60
Squalene	410.72	0	0	9.38	1	15	0.00
Gentamicin (control)	477.60	12	8	-2.15	2	7	199.73
Fluconazole (control)	306.27	7	1	0.88	0	5	81.65
Butylhydroxyanisole (control)	180.24	2	1	2.66	0	2	29.46
Celecoxib (control)	381.37	7	1	3.40	0	4	86.36

MW: Molecular weight; HBA: Hydrogen bond acceptor; HBD: Hydrogen bond donor; Log P, lipophilicity; nRB: number of rotatable bonds; TPSA: topological polar surface area.

Toxicity Prediction

Table 4 presents the predicted activity or inactivity of the identified phytocompounds from *A. wilkesiana* leaf extract with respect to toxicity parameters. These include liver toxicity and several toxicity endpoints such as mutagenicity, carcinogenicity, immunotoxicity, and hepatotoxicity. The table also indicates the assigned toxicity for each identified phytocompound.

Table 4: Toxicological properties of identified compounds from *A. wilkesiana* leaf.

Compounds	Mutagenicity	Carcinogenicity	Immunotoxicity	Hepatoxicity	Toxicity Class
4-Heptafluorobutyryloxyhexadecane	Inactive	Inactive	Inactive	Inactive	V
Naphthalene, decahydro-, trans-	Inactive	**Active**	Inactive	Inactive	VI
Naphthalene, decahydro-2-methyl-	Inactive	Inactive	Inactive	Inactive	VI
Epinephrine	Inactive	Inactive	Inactive	Inactive	I
7-Methyl-Z-tetradecen-1-ol acetate	Inactive	**Active**	Inactive	Inactive	V
Oxalic acid, 3,5-difluorophenyl tetradecyl ester	Inactive	Inactive	**Active**	Inactive	V
Aspidospermidin-17-ol, 1-acetyl-19,21-epoxy-15,16-dimethoxy-	Inactive	Inactive	**Active**	Inactive	IV
Oleic Acid	Inactive	Inactive	Inactive	Inactive	II
7,9-Di-tert-butyl-1-oxaspiro(4,5)deca-6,9-diene-2,8- dione	Inactive	Inactive	Inactive	Inactive	IV
Dibutyl phthalate	Inactive	**Active**	Inactive	Inactive	V
Cyclotetradecane, 1,7,11-trimethyl-4-(1-methylethyl)-	Inactive	Inactive	Inactive	Inactive	III
Bis(tridecyl) phthalate	Inactive	**Active**	Inactive	Inactive	IV
Squalene	Inactive	Inactive	Inactive	Inactive	V
Gentamicin (control)	Inactive	Inactive	**Active**	Inactive	V
Fluconazole (control)	Inactive	Inactive	Inactive	**Active**	IV
Butylhydroxyanisole (control)	Inactive	**Active**	Inactive	Inactive	IV
Celecoxib (control)	Inactive	**Active**	Inactive	Inactive	IV

Class 1: May be fatal if swallowed ($LD_{50} \leq 5$mg/kg); Class 2: May be fatal if swallowed (5mg/kg < $LD_{50} \leq 50$mg/kg); Class 3: May be toxic if swallowed (50mg/kg < $LD_{50} \leq 300$mg/kg); Class 4: May be harmful if swallowed (300mg/kg < $LD_{50} \leq 2000$mg/kg); Class 5: May be harmful if swallowed (2000mg/kg < $LD_{50} \leq 5000$mg/kg); Class 6: May be non-toxic ($LD_{50} \leq 5000$mg/kg)

Discussion

The GC-MS analysis of the ethanolic extract of *Acalypha wilkesiana* leaf revealed a complex phytochemical profile, identifying 62 compounds comprising several classes, including alkanes, alkenes, fatty acids, terpenoids, alkaloids, esters, and various halogenated hydrocarbons. The most abundant compound identified was the triterpene, squalene (21.13%), followed by the monounsaturated fatty acid, 9-octadecenoic acid (oleic acid) (17.62%) and the long-chain aldehyde, 13-octadecenal, (Z)- (16.63%). The predominance of squalene is particularly noteworthy, as this triterpene has been identified as an antioxidant and chemopreventive agent, known to inhibit carcinogenesis (Akubugwo *et al.*, 2022). Its high concentration in the leaf extract indicates a significant role in the plant's defense mechanisms and suggests its potential for nutraceutical applications. Similarly, oleic acid, the most abundant fatty acid in the extract, is recognized for its broad spectrum of bioactivity, including antimicrobial, anti-inflammatory, and antioxidant effects (Ralte *et al*., 2022). The extract also contained a substantial proportion of other bioactive lipids. The long-chain aldehydes, such as, 13-octadecenal, and E-15-heptadecenal, are known to contribute to the characteristic aroma of plants but are also increasingly recognized for their antimicrobial and cytotoxic activities (Ajanaku *et al.*, 2018; Sanjaya and Lekha, 2019). Furthermore, the identification of 7,9-Di-tert-butyl-1-oxaspiro(4,5)deca-6,9-diene-2,8-dione, spiro-lactone derivative, is significant, as this compound has been reported to exhibit antioxidant and anti-inflammatory properties (Tsochatzis *et al.*, 2020; Mathe and Karlapudi, 2025). The chemical profile observed in this study shows some similarities with a recent study on the methanol extract of *A. wilkesiana* leaf (Idowu and Edwor, 2025).

To corroborate the experimental findings and predict the potential mechanisms of action, the major phytoconstituents identified by GC-MS were subjected to molecular docking against targeted proteins associated with antimicrobial, antioxidant, and anti-inflammatory pathways. Among the screened compounds, Aspidospermidin-17-ol, 1-acetyl-19,21-epoxy-15,16-dimethoxy- demonstrated the most promising broad-spectrum activity, exhibiting the highest binding affinities against bacterial (8FJC; -7.8 kcal/mol), antioxidant (2HE3; -6.9 kcal/mol), and pro-inflammatory (3NTG; -7.6 kcal/mol) targets. The consistent bioactivity of this compound is further supported by Nwofor *et al*. (2025), who reported that aspidospermidin-17-ol, 1-acetyl-19,21-epoxy-15,16-dimethoxy- isolated from the red variant of *A. wilkesiana* exhibited a superior binding affinity against fungal proteins, outperforming both Ketoconazole and the co-crystallized ligand. Analysis of the 2D interaction revealed that the high affinity of this alkaloid for the bacterial protein 8FJC is due to hydrogen bonding with key residues, such as GLU-489 and GLN-566, within the catalytic pocket of GtfB. These interactions suggest a potential capacity to interfere with glucan synthesis, a critical step in the formation of dental plaque biofilms by *Streptococcus mutans* (Xu *et al.*, 2018). Conversely, Cyclotetradecane, 1,7,11-trimethyl-4-(1-methylethyl)- showed the highest affinity for 4M8I. Its 2D interaction indicates that its hydrophobic structure fits deeply into a lipophilic pocket, forming strong alkyl interactions with PHE-144 and PHE-258. Epinephrine showed moderate binding to the antioxidant protein 2HE3 (-5.2 kcal/mol). The 2D interaction diagram revealed that the catechol moiety forms hydrogen bonds with TYR-125 and ARG-168, along with a π-alkyl interaction with ARG-167, which may contribute to stabilization of the ligand within the binding pocket. Squalene, the most abundant compound in the extract, exhibited the second-highest binding affinity against 3NTG. Its 2D interaction diagram showed that it did not form hydrogen bonds with COX-2 (PDB ID: 3NTG), and its interaction with the enzyme was primarily mediated through hydrophobic contacts within the catalytic pocket. The hydrophobic effect plays a significant role in protein–ligand binding. Binding pockets enriched with hydrophobic substituents are often associated with improved binding energy, as increased hydrophobic contacts within the drug–target interface can enhance ligand affinity and contribute to the biological activity of the compound (Daze and Hof, 2016; Prabhavathi *et al.*, 2020). This observation is consistent with the lipophilic nature of triterpenes, such as Squalene, which are known to exert anti-inflammatory effects,in part, through enzyme inhibition (Ibrahim and Naina Mohammed, 2021).

To assess the pharmacokinetic potential of the identified phytocompounds, their drug-likeness was evaluated using Lipinski's Rule of Five and Veber's rules. These parameters predict oral bioavailability based on molecular weight (MW ≤ 500 g/mol), hydrogen bond acceptors (HBA ≤ 10), hydrogen bond donors (HBD ≤ 5), lipophilicity (Log*P* ≤ 5), and Veber's criteria of rotatable bonds (nRB ≤ 10) and topological polar surface area (TPSA ≤ 140 Å²). According to these rules, a compound or potential medicinal agent cannot violate all parameters while still demonstrating good oral bioavailability (Li *et al*., 2003; Duffy and Shields, 2015). Among the evaluated compounds, epinephrine, aspidospermidin-17-ol, 1-acetyl-19,21-epoxy-15,16-dimethoxy-, 7,9-Di-tert-butyl-1-oxaspiro(4,5)deca-6,9-diene-2,8-dione, and dibutyl phthalate demonstrated excellent compliance with Lipinski's rules, exhibiting zero violations. Bis(tridecyl) phthalate recorded two violations due to its high molecular weight (530.82 g/mol) and elevated Log*P* (9.90). All compounds except 4-heptafluorobutyryloxyhexadecane, oxalic acid, 3,5-difluorophenyl tetradecyl ester, 7-methyl-z-tetradecen-1-ol acetate, oleic acid, and squalen**e** demonstrated excellent compliance to Veber's rules.

The selected phytocompounds from *Acalypha wilkesiana* were also evaluated for mutagenicity, carcinogenicity, immunotoxicity, hepatotoxicity, and assigned a toxicity class (Class I - VI). None of the phytocompounds were predicted to be hepatotoxic or mutagenic. However, naphthalene, decahydro-, trans-, 7-methyl-Z-tetradecen-1-ol acetate, dibutyl phthalate, and bis(tridecyl) phthalate were predicted to be carcinogenic. For the phthalate derivatives, this aligns with existing literature, which highlights concerns about their potential adverse health effects, including endocrine and reproductive toxicity (Casale and Rice, 2023). Additionally, oxalic acid, 3,5-difluorophenyl tetradecyl ester, and aspidospermidin-17-ol, 1-acetyl-19,21-epoxy-15,16-dimethoxy-, were predicted to be immunotoxic. Notably, aspidospermidin-17-ol demonstrated strong binding affinities across multiple targets; however, its predicted immunotoxicity suggests that, despite its promising bioactivity, its potential effects on the immune system warrant further investigation through *in vitro* and *in vivo* studies. All compounds fell within Classes IV - VI, indicating low to no predicted toxicity. However, epinephrine was classified as Class I, which indicates high toxicity. This observation is consistent with its known pharmacological profile, as epinephrine is a potent therapeutic agent with significant physiological effects even at low concentrations and is therefore administered with caution due to potential complications at higher doses (Kanwar *et al*., 2010).

Conclusion

This study focused on the comprehensive identification of bioactive compounds present in *Acalypha wilkesiana* leaf extract using GC-MS analysis. Among the bioactive compounds identified, aspidospermidin-17-ol, 1-acetyl-19,21-epoxy-15,16-dimethoxy-, 7,9-di- tert-butyl-1-oxaspiro(4,5)deca-6,9-diene-2,8-dione, oxalic acid, 3,5-difluorophenyl tetradecyl ester, cyclotetradecane, 1,7,11-trimethyl-4-(1-methylethyl)-, oleic acid, naphthalene, decahydro- trans-, squalene, 4-heptafluorobutyryloxyhexadecane, bis(tridecyl)phthalate, naphthalene, decahydro-, trans-, and epinephrine, displayed promising binding affinity towards different proteins through molecular docking studies. Additionally, their drug-like features were demonstrated, indicating their potential suitability for drug development. The *in silico* potentials of the phytochemicals identified provide a scientific basis for the widespread traditional use o*f Acalypha wilkesiana* leaf and suggest that these compounds may contribute to its reported effectiveness in the management of toothache and other oral inflammatory conditions.

References

Akubugwo, E.I., Emmanuel, O., Ekweogu, C.N., Ugbogu, O.C., Onuorah, T.R., Egeduzu, O.G. and Ugbogu, E.A. (2022). Analysis of the phytochemical constituents, safety assessment, wound healing and anti-inflammatory activities of *curcubita pepo* leaf extract in rats. *Scientia Pharmaceutica*, **90**:64

Bowen, W. H. & Koo, H. (2011). Biology of *Streptococcus mutans*-derived glucosyltransferases: Role in extracellular matrix formation of cariogenic biofilms. *Caries Research*, 45, 69–86. https://doi.org/10.1159/000324598

Casale, J. & Rice, A. S. (2023). Phthalates toxicity. In *StatPearls*. StatPearls Publishing.

Daze, K. & Hof, F. (2016). Molecular interaction and recognition. In *Encyclopedia of physical organic chemistry* (Vol. 5). Wiley. https://doi.org/10.1002/9781118468586.epoc3001

Duffy, F. J., Devocelle, M. & Shields, D. C. (2015). Computational approaches to developing short cyclic peptide modulators of protein–protein interactions. *Methods in Molecular Biology*, 1268, 241–271.

Ibrahim, N. I. & Naina Mohamed, I. (2021). Interdependence of anti-inflammatory and antioxidant properties of squalene—Implication for cardiovascular health. *Life*, 11(2), 103. https://doi.org/10.3390/life11020103

Idowu, A. A. & Edewor, T. I. (2025). Phytochemical profile and antioxidant activity of *Acalypha wilkesiana* leaves. *International Journal of Chemistry and Chemical Processes, 11*(1), 57-73

Isola, G. (2020). Current evidence of natural agents in oral and periodontal health. *Nutrients*, 12, 585. https://doi.org/10.3390/nu12020585

Kanwar, M., Irvin, C.B., Frank, J.J., Weber, K.and Rosman, H. (2010). Confusion about epinephrine dosing leading to iatrogenic overdose: A life-threatening problem with a potential solution. *Annual Emergency Medicine*, **55**(4): 341-344

Kouidhi, B., Zmantar, T. and Bakhrouf, A.V. (2010). Anticariogenic and cytotoxic activity of clove (*Eugenia caryophyllata*) essential oil against a large number of oral pathogens. *Annual Review of Microbiology*, **60**:599–604

Li, F., Yin, Y., Tan, B., Kong, X. and Wu, G. (2011). Leucine nutrition in animals and humans: mTOR signaling and beyond. *Amino Acids*, **41**:1185-1193.

Li, J. J., Holsworth, D. D. & Hu, L. Y. (2003). Molecular properties that influence the oral bioavailability of drug candidates. *Chemtracts*, 16(7), 439–442.

Lipinski, C.A., Lombardo, F., Dominy, B.W. and Feeney, P.J. (2001). Experimental and computational approaches to estimate solubility and permeability in drug discovery and development settings. *Advanced Drug Delivery Review*, **46**:3-26

Mathe, A. & Karlapudi, A. P. (2025). Computational and experimental evaluation of a dual COX inhibitor: Insights from DFT, molecular simulations, and in-vitro validation. *Letters in Drug Design & Discovery*, *22*(2), Article 100009. https://doi.org/10.1016/j.lddd.2025.100009

Mi, N., Zhang, M., Ying, Z., Lin, X. & Jin, Y.(2024). Vitamin intake and periodontal disease: A meta-analysis of observational studies. *BMC Oral Health*, 24, 117. https://doi.org/10.1186/s12903-024-03850-5

Milutinovici, R. A., Chioran, D., Buzatu, R., Macasoi, I., Razvan, S., Chioibas, R., Corlan, I. V., Tanase, A., Horia, C., Popovici, R. A., et al. (2021). Vegetal compounds as sources of prophylactic and therapeutic agents in dentistry. *Plants*, 10, 2148. https://doi.org/10.3390/plants10102148

Moghadam, E. T., Yazdanian, M., Tahmasebi, E., Tebyanian, H., Ranjbar, R., Yazdanian, A., Seifalian, A. & Tafazoli, A. (2020). Current herbal medicine as an alternative treatment in dentistry: In vitro, in vivo and clinical studies. *European Journal of Pharmacology*, 889, 173665. https://doi.org/10.1016/j.ejphar.2020.173665

Nwofor, O. K. & Duru, C. E. (2025). In-vitro, bioinformatics and computational biophysical analyses of antifungal phytochemicals from *Acalypha wilkesiana* variants targeting *Malassezia* lipase. *Tropical Journal of Drug Research, 2*(9), 231–244. https://doi.org/10.26538/tjdr/v2i9.3

Nwolisah, O. S., Enemor, V. H. A., Odili, C. E., Ehichanya, C. A., Obih, M. S. & Okochi, C. V. (2024). Evaluation of the proximate, mineral and vitamin compositions of *Acalypha wilkesiana* leaf. *The Bioscientist Journal, 12*(1), 87–97.

Prabhavathi, H., Dasegowda, K. R., Renukananda, K. H., Lingaraju, K. & Naika, H. R. (2020). Exploration and evaluation of bioactive phytocompounds against BRCA proteins by in silico approach. *Journal of Biomolecular Structure and Dynamics*, 1–15. https://doi.org/10.1080/07391102.2020.1790424

Ralte, L., Khiangte, L., Thangjam, N.M., Kumar, A. and Singh, Y.T. (2022). GC-MS and molecular docking analyses of phytochemicals from the underutilized plant, *Parkia timoriana* revealed candidate anti-cancerous and anti-inflammatory agents. *Nature*, **12**:3395

Sanjaya, P. and Lekha, K. (2019). Preliminary phytochemical analysis, GC-MS studies and antioxidant activity of *Majidea zangueberica* J. Kirk leaf extracts. *Journal of medicinal plant studies*, **7**(2): 186-195

Tsochatzis, E.D., Gika, H. & Theodoridis, G. (2020). Development and validation of a fast gas chromatography mass spectrometry method for the quantification of selected non-intentionally added substances and polystyrene/polyurethane oligomers in liquid food simulants. *Analytica Chimica Acta, 1130*, 49–59. https://doi.org/10.1016/j.aca.2020.06.049

Ustianowski, Ł., Ustianowska, K., Gurazda, K., Rusiński, M., Ostrowski, P. & Pawlik, A. (2023). The role of vitamin C and vitamin D in the pathogenesis and therapy of periodontitis—Narrative review. *International Journal of Molecular Sciences*, 24(7), 6774. https://doi.org/10.3390/ijms24076774

Veber, D.F., Johnson, S.R., Cheng, H.Y., Smith, B.R. and Ward, K.W. (2002). Molecular properties that influence the oral bioavailability of drug candidates. *Journal of Medicinal Chemistry*, **45(12)**: 2615-2623

Xu, R.R., Yang, W.D., Niu, K.X., Wang, B. and Wang, W.M. (2018). An update on the evolution of glucosyltransferase (Gtf) genes in *Streptococcus*. Frontiers of Microbiology, **9**:297